

See discussions, stats, and author profiles for this publication at: <https://www.researchgate.net/publication/258630724>

# Real-Time Monitoring of Transesterification by $^1\text{H}$ NMR Spectroscopy: Catalyst Comparison and Improved Calculation for Biodiesel Conversion

ARTICLE in ENERGY & FUELS · SEPTEMBER 2012

Impact Factor: 2.79 · DOI: 10.1021/ef301035s

---

CITATIONS

3

---

READS

132

2 AUTHORS, INCLUDING:



[Lisa A. Anderson](#)

Massachusetts Institute of Technology

8 PUBLICATIONS 100 CITATIONS

SEE PROFILE

# Real-Time Monitoring of Transesterification by $^1\text{H}$ NMR Spectroscopy: Catalyst Comparison and Improved Calculation for Biodiesel Conversion

Lisa A. Anderson and Annaliese K. Franz\*

Department of Chemistry, University of California, One Shields Avenue, Davis, California 95616, United States

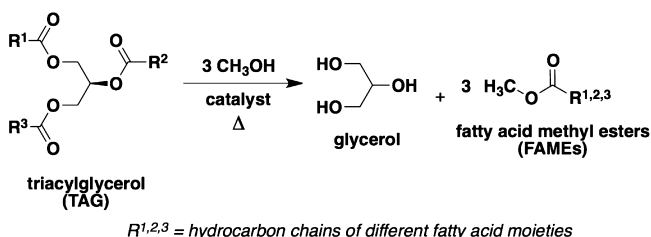
## S Supporting Information

**ABSTRACT:** A facile, rapid, and noninvasive method for monitoring transesterification of acylglycerols for the application of biodiesel production is reported. High-field NMR spectroscopic analysis prevents incorrect and overintegration of signals that have previously been combined due to crowding on low-field NMR spectrometers. Using high resolution NMR, a new and more accurate equation utilizing a nonoverlapping signal is presented for calculating biodiesel conversion. Here, we demonstrate the kinetic acquisition of high-resolution NMR spectra for real-time monitoring of the consumption and formation of triacylglycerols, diacylglycerols, and fatty acid methyl esters in biodiesel production. This method of reaction monitoring takes place on small scale in a standard NMR tube, is acquired with existing laboratory instruments, and avoids taking aliquots from a reaction. By comparing different catalysts and conditions, this method facilitates the selection/optimization of catalysts and may improve quality in compliance with fuel standards by assessing the reaction composition for models of an industrial transesterification system. Using this method,  $\text{H}_2\text{SO}_4$ ,  $\text{NaOH}$ , and 1,5,7-triazabicyclo[4.4.0]dec-5-ene (a bifunctional, nonionic base) have been compared as catalysts for transesterification.

## INTRODUCTION

Reducing dependence on petroleum-based fuels is of current interest due to negative effects of fossil fuels such as increasing crude oil prices, increasing energy consumption, and climate change.<sup>1,2</sup> Biodiesel, a renewable liquid fuel composed of fatty acid alkyl esters (FAAEs), is a feasible replacement for petroleum-based fuel and can be burned directly in currently existing diesel engines. The FAAEs that comprise biodiesel are produced upon transesterification of animal, plant, or algae oils in the presence of an alcohol and a catalyst (Scheme 1).<sup>3,4</sup>

**Scheme 1. Reaction Scheme for the Transesterification of TAGs to Biodiesel**



Feedstock oils for biodiesel contain mixtures of acylglycerols, mostly triacylglycerols (TAGs), with varying fatty acid chain lengths and degrees of unsaturation (Supporting Information, Figure S1). Transesterification is a progression of three successive, reversible reactions containing triacylglycerols (TAGs), diacylglycerols (DAGs), monoacylglycerols (MAGs), FAAE, and glycerol as components.<sup>5</sup> Unconverted TAG, intermediate DAG and MAG, and byproducts such as free fatty acids and glycerol may be present as undesirable residues due to partial conversion or insufficient purification of reaction

mixtures. Upon combustion, trace concentrations of residual contaminants that are not removed from washing can influence the low temperature performance of biodiesel and can lead to engine problems and hazardous emissions.<sup>6</sup> The ASTM (American Society for Testing and Materials) standard D7651 for biodiesel limits the levels of free glycerol to 0.02% and total glycerol (including acylglycerols) to 0.25%.<sup>7,8</sup> Therefore, it is necessary to control and monitor the presence of undesirable residues that may arise during transesterification to ensure the efficient conversion and quality of biodiesel.

Previous reports have monitored the production of acylglycerols, FAAEs, and byproducts using  $^1\text{H}$  NMR spectroscopy<sup>9–15</sup> and  $^{13}\text{C}$  NMR spectroscopy<sup>16–19</sup> in conjunction with equations, calibration curves, and internal standards. Other analytical methods and comparisons<sup>20–22</sup> have also been reported, which include but are not limited to, gas chromatography (GC),<sup>23,24</sup> UV–vis spectrometry, high pressure liquid chromatography (HPLC),<sup>25,26</sup> and Fourier transform infrared spectroscopy (FTIR).<sup>20,21,27</sup> Only a few reports use direct real-time monitoring of the transesterification process.<sup>28,29</sup>  $^1\text{H}$  NMR spectroscopy is a robust, rapid, and quantitative tool that can be applied for determining the presence of multiple chemical species and monitoring transesterification reactions over time based on the integration of individual proton signals. Previous methods utilizing NMR spectroscopic monitoring of transesterification require removal of aliquots from a larger reaction, which can be tedious, and incomplete quenching can lead to inaccurate assessment of reaction progression. Furthermore, analysis of aliquots does not

Received: June 19, 2012

Revised: September 7, 2012

Published: September 11, 2012



allow for direct real-time monitoring of intermediate species (i.e., DAGs and MAGs) formed in the transesterification process. With increasing biodiesel production and use, there is a growing need to utilize and improve technologies for correctly analyzing biodiesel synthesis and properties.<sup>30,31</sup>

When monitoring the transesterification process using NMR spectroscopy, it is important to recognize the effect of NMR field strength on the accuracy of conversion calculations. Recently, a comparison was published between the two most prominent NMR spectroscopy methods and equations used for measuring conversion of the transesterification reaction.<sup>32</sup> Andrade et al. assessed the uncertainties resulting from correlating the two methods. However, one of these methods utilizes an incorrect calculation based on the assignment of peaks in the Knothe equation. The Knothe equation ( $C_K$ , eq 1,  $I_{ME}$  = integration of methyl ester, and  $I_{TG}$  = integration of TAG glyceryl methylenes)<sup>10</sup> integrates the glyceryl methylenes of the diminishing TAG at 4.10–4.33 ppm, and the Gelbard equation ( $C_G$ , eq 2,  $I_{ME}$  = integration of methyl ester, and  $I_{CH_2}$  = integration of methylenes  $\alpha$  to a carbonyl)<sup>9</sup> integrates the methylenes  $\alpha$  to the carbonyl of all fatty acid chains at 2.31 ppm. Both equations use the singlet methyl ester peak of the product at 3.67 ppm. Knothe incorrectly assigned five protons to the glyceryl methylenes instead of four protons due to the lack of resolution in the spectra. Although there are five glyceryl protons total, the signal for the glyceryl methine lies downfield at 5.27 ppm. In both equations, these signals can overlap with other reaction components, which can lead to miscalculated conversion and sample composition if not integrated correctly. For example, the signal at 2.31 ppm can overlap with protons from FFA (if present),<sup>33</sup> and the signals from 4.10 to 4.33 ppm can overlap with acylglycerol intermediates (vide infra). Although many works have recognized this error and have adjusted their calculations,<sup>11</sup> there are still many recent reports that continue to use the incorrect equation based on the incorrect assignment (i.e., integration) of peaks.

$$C_K = 100 \times \left( \frac{5I_{ME}}{5I_{ME} + 9I_{TG}} \right) \quad (1)$$

$$C_G = 100 \times \left( \frac{2I_{ME}}{3I_{CH_2}} \right) \quad (2)$$

Herein, a method is described that utilizes NMR spectroscopic time-array acquisition to monitor the transesterification process for the production of biodiesel in real-time. The use of reaction monitoring by NMR spectroscopy has increased over the past decade,<sup>34</sup> with applications in pharmaceutical research, reaction kinetics, and characterizing multicomponent reaction mixtures.<sup>35,36</sup> The advances in online monitoring, NMR data processing, and use of benchtop spectrometers also contribute to the development of these methods for broad applications.<sup>37,38</sup> However, the kinetic acquisition of high-resolution NMR has not previously been used to monitor biodiesel production. We demonstrate the utility of monitoring the biodiesel production where high-resolution NMR spectra enhance the ability to monitor intermediates (e.g., DAGs) in a complex reaction mixture. We also present advances comparing fatty acid methyl ester (FAME) conversion using an improved conversion equation, the effect of resolution on apparent conversion, monitoring intermediates under different reaction conditions, and comparing transesterification catalysts using real-time NMR spectro-

scopic monitoring. From a practical standpoint, this method utilizes commonly existing laboratory spectrometers with no modification in instrumentation necessary. Catalyst systems compared here include  $H_2SO_4$  (a Brønsted acid), NaOH (a Brønsted base), and 1,5,7-triazabicyclo[4.4.0]dec-5-ene (a bifunctional, nonionic base). Using direct real-time monitoring of the transesterification process to compare these catalysts demonstrates that 1,2-DAGs are a prominent intermediate observed during the transesterification catalyzed by  $H_2SO_4$  but are not commonly observed when NaOH or 1,5,7-triazabicyclo[4.4.0]dec-5-ene is used.

## ■ EXPERIMENTAL PROCEDURES

**Oils and Reagents.** Olive oil (purified/refined) was purchased from Acros Organics (Morris Plains, NJ). 1,3-diolein and 1,2-diolein were purchased from MP biomedical (Solon, OH). 1-Oleoyl-*rac*-glycerol, 2-oleoyl-glycerol, and 1,5,7-triazabicyclo[4.4.0]dec-5-ene (TBD) were purchased from Sigma-Aldrich (St. Louis, MO). Deuterated chloroform ( $CDCl_3$ ) with tetramethylsilane (TMS, v/v 0.05%) was purchased from Cambridge Isotope Laboratories (Andover, MA). Standard 5 mm NMR tubes (Wilmad Labglass, Vineland, NJ) were used for NMR spectroscopy experiments. Methanol,  $H_2SO_4$ , and  $CHCl_3$  were purchased from Fisher Scientific (Fairlawn, NJ). A 30:1 molar ratio of  $CH_3OH$ /oil was used for all experiments. Anhydrous methanol was used, except where the use of reagent-grade (i.e., nonanhydrous) methanol is indicated.

**$^1H$  NMR Spectroscopy.** Spectra for the comparison of NMR spectral resolution were acquired using Mercury 300, Inova 400, VNMRs 600 (Varian, Palo Alto, CA), and Avance 800 (Bruker, Germany) MHz spectrometers. Oil was dissolved to a concentration of 20 mg/mL in  $CDCl_3$  and transferred to a 5 mm NMR tube. Spectra were acquired at 298 K for the indicated number of scans, with a relaxation delay of 1 s, pulse angle of 45°, 32K data points, and line broadening of 0.2 Hz. For relaxation delay experiments, relaxation times were changed while all other parameters were constant. Figures were processed using MestReNova software (Mestrelab Research, SL, Santiago de Compostela, Spain). TMS (v/v 0.05%) was used as an internal reference and chemical shifts were assigned based on previous reports<sup>39</sup> and comparison to standards.

$^1H$  NMR time-array experiments were performed either at 23 °C (room temperature) or at 60 °C with a VNMRs 600 MHz spectrometer (Varian, Palo Alto, CA). Reagents were added directly to the NMR tube before acquisition with the catalyst added as quickly as possible. The tube was capped with a polyethylene gastight tube cap (5 mm, Superior Pressure Tube Cap, Wilmad Labglass, Buena, NJ) and sealed with parafilm to prevent evaporation. A mock sample was used to lock and shim before beginning the time-array experiment. Time-array spectra were acquired at indicated time interval and temperature with automated VNMRJ 2.2 D software (Varian systems, Yarnton, Oxford, U.K.). Data were processed with MestReNova 7.1 (Mestrelab Research, SL, Santiago de Compostela, Spain) with phase correction and Bernstein polynomials baseline correction. Spectra from the kinetic data were integrated with MestReNova advanced data analysis tool. Using eq 3, the total amount of FAME was determined and normalized to 100 with the other components present to achieve conversion by percent of total (e.g., TAG, DAG, and FAME total). Plots were made with Microsoft Excel (Microsoft Office 2011, version 14.2.2).

**Comparison of NMR vs Bench-Scale Reaction.** To compare NMR reaction results to a larger scale reaction, 500 mg benchtop flask/vial reactions were performed in screw-capped vials while stirring at 60 °C. All reagents were scaled appropriately, maintaining a 30:1 molar ratio of  $CH_3OH$ /oil. 1 mL aliquots were removed for the bench-scale reaction with chloroform and 50  $\mu$ L aliquots were removed for the bench-scale reaction without chloroform.

## ■ RESULTS AND DISCUSSION

### Importance of NMR Field Strength and Parameters for Calculating Transesterification Conversion.

Close proximity of the chemical shifts for the TAG glyceryl methine and olefinic protons may lead to incorrect integration of the two separate types of protons when lower field NMR spectrometers are employed. As shown in Figure 1a, the

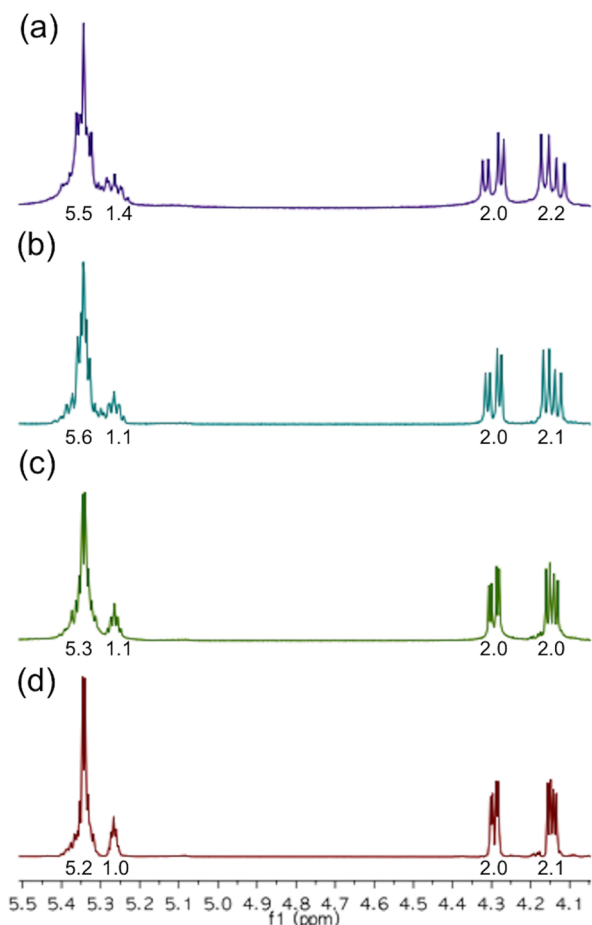


**Figure 1.**  $^1\text{H}$  NMR spectra of olive oil (16 scans,  $\text{CDCl}_3$ , 20 mg/mL) using (a) 300 MHz, (b) 400 MHz, (c) 600 MHz, or (d) 800 MHz spectrometers. Expansion shows a 4.0–5.5 ppm region. Chemical shifts: glyceryl methylenes (4H, 4.10–4.33 ppm), glyceryl methine (1H, 5.27 ppm), olefinic protons (5.34 ppm). The glyceryl methylene at 4.3 ppm is normalized to 2H. Integration values are indicated underneath each signal.

glyceryl methine (at 5.27 ppm) can overlap with the olefinic protons (at 5.34 ppm), making it difficult to accurately distinguish integration between the two signals. Inaccurate integration alters the calculated conversion such that incorrect conversions and assessment of the reaction mixture can occur. However, with higher field instruments, the glyceryl methine peak can be resolved, resulting in two distinct signals for the calculation of more accurate conversions (Figure 1b–d). At a higher magnetic field, signals are spread over a larger frequency and linewidths decrease when signals are adjusted to ppm. Thus, signals can be more readily distinguished using a higher field instrument. In addition, there is a gain in sensitivity and faster measurement that is attributed to a greater population difference in spin states and increase in the signal-to-noise ratio.

Because the methylene signals from 1,2-DAG, 1,3-DAG, and 1-MAG overlap in the same region as the TAG methylene signals, these signals should be taken into account when calculating conversion of TAG to FAME. DAGs and MAGs are produced as intermediates during the methanolysis of TAGs to FAMEs, and these species must be quantified to accurately assess conversion. TAGs, DAGs, and MAGs all have distinct, characteristic glyceryl methine signals as observed by  $^1\text{H}$  NMR spectroscopy (Table 1 and Figure 2). The DAG glyceryl

**Table 1.** Acylglycerol  $^1\text{H}$  NMR Chemical Shift Assignments (TAG, DAG, and MAG species)

molecule	glyceryl protons	$\delta$ (ppm) <sup>a</sup>	carbon number
TAG	–CH–	5.23–5.30 (q)	C2
1,2-DAG	–CH–	5.02–5.11 (q)	C2
2-MAG	–CH–	4.90–4.96 (q)	C2
TAG	–CH <sub>2</sub> –	4.27–4.33 (dd), H <sub>a</sub> ; 4.11–4.17 (dd), H <sub>b</sub>	C1 (H <sub>a</sub> and H <sub>b</sub> ) and C3 (H <sub>a</sub> and H <sub>b</sub> )
1,2-DAG	–CH <sub>2</sub> –	4.17–4.29 (m)	C1 and C3
1-MAG	–CH <sub>2</sub> –	4.15–4.25 (dd)	C2
1,3-DAG	–CH <sub>2</sub> –	4.11–4.22 (dd and dd)	C1 and C3
1,3-DAG	–CH–	4.06–4.12 (q)	C2
2-MAG	–CH <sub>2</sub> –	3.80–3.86 (bm)	C1 and C3
1-MAG	–CH <sub>2</sub> –	3.56–3.72 (dd)	C3
1-MAG	–CH–	3.90–3.96 (q)	C1

<sup>a</sup>s = singlet, t = triplet, q = quintet, m = multiplet, dd = doublet of doublets, bm = broad multiplet.

methylene and methine peaks shift in the NMR spectra with the methine changing from 5.27 ppm to 5.08 ppm for the 1,2-DAG and 4.08 ppm for the 1,3-DAG. The entire region from 4.10 to 4.33 ppm should be integrated to include methylene protons from all intermediates in the conversion process, but with care to not include any glyceryl methine protons, which can also overlap in this region. Intermediate components, such as DAGs, can be detected down to 0.2 mg (1%) by  $^1\text{H}$  NMR spectroscopy (Supporting Information, Table S1). The presence of FFA should also be considered, particularly when using strong alkali catalysts that promote saponification, such as NaOH, and can be calculated using the chemical shift of the unmerged FA  $\alpha$  methylene at 2.38 ppm.<sup>33</sup>

The overlapping methylene signals of acylglycerol intermediates (Figure 2) emphasize the importance of utilizing higher resolution NMR instruments to distinguish the olefinic protons (5.35 ppm) from the glyceryl methine (5.27 ppm) for accurate calculated conversion. Reported chemical shifts of TAGs and fatty acid methyl esters (FAMEs) are shown in the Supporting Information, Table S2. By comparing the integration of triacylglycerol and methyl ester proton signals, conversion can be determined. Andrade et al. compared the conversion of seven different oils (soybean, corn, sunflower, canola, linseed, cottonseed, and jatropha)<sup>32</sup> using  $^1\text{H}$  NMR spectroscopy where all signals representing the olefinic protons and glyceryl methine are grouped into one integrated signal with a chemical shift of 5.30 ppm.<sup>32</sup> Previous reports for TAG structure and chemical shift tables indicate that the glyceryl methine is at a different chemical shift than the glyceryl methylenes, but the spectra integrals fail to distinguish between the two.<sup>10</sup> Given the possible presence of DAG and MAG signals underneath the TAG methylene region, up to 38% of conversion can be overestimated when the total area between



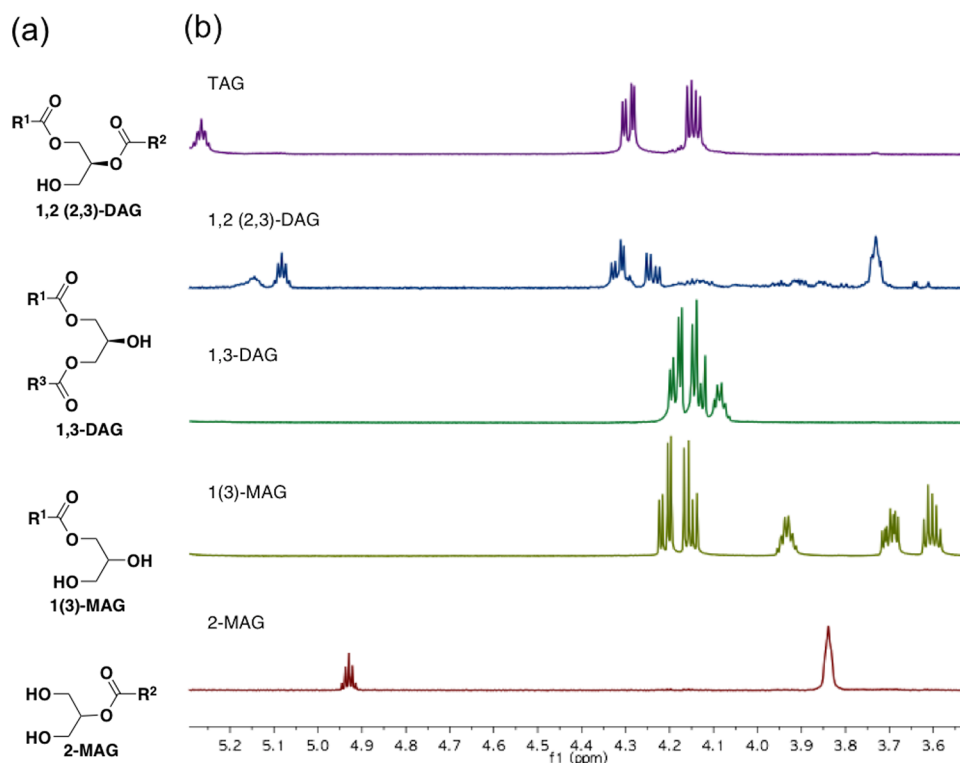


**Figure 2.** (a) Structures of acylglycerols present during transesterification (see Scheme 1 for TAG) and (b) expansion of <sup>1</sup>H NMR spectra (600 MHz, 16 scans, CDCl<sub>3</sub>) for TAG (olive oil), 1,2 (2,3)-DAG (1,2-dioleoyl-rac-glycerol), 1,3-DAG (1,3-diolein), 1(3)-MAG (1(3)-oleoyl-rac-glycerol), and 2-MAG (2-oleoyl-glycerol). Peak height normalization based on glyceryl methines.

4.10 and 4.33 ppm is integrated to 5H (Supporting Information, Table S3 and Figure S2).

We propose a new equation for calculating biodiesel conversion that utilizes the TAG glyceryl methine signal at 5.27 ppm. With high resolution NMR, the acylglycerol methine signals are distinctive for each molecule in the NMR spectra and can provide accurate quantitation. Therefore, we suggest a new equation to calculate conversion using the signal of the FAME methyl at 3.67 ppm with the signal of the TAG glyceryl methine at 5.27 ppm, which contains no underlying signals from other reaction components ( $C_F$ , eq 3, where  $I_{ME}$  = integration of methyl ester and  $I_{TM}$  = integration of TAG glyceryl methine). This new equation avoids overlapping signals and the possibility of inaccurate integration that can effect conversion calculations. A sample comparison of calculated conversions using eq 1, eq 2, and eq 3 is provided in the Supporting Information (Tables S3 and Figure S2).

$$C_F = 100 \times \left( \frac{I_{ME}}{I_{ME} + 9I_{TM}} \right) \quad (3)$$

The effect of relaxation delay time on quantification by NMR spectroscopy was investigated to ensure accuracy for real-time NMR reaction monitoring. Mambrini et al. recently reported the longitudinal relaxation time ( $T_1$ ) with a 400 MHz spectrometer for biodiesel to be 2.35 s.<sup>40</sup> Using diffusion coefficient-formula weight correlation analysis by diffusion ordered NMR spectroscopy (DOSY), Socha et al. observed the slowest spin-diffusion rate with triolein and the fastest with methyl ester.<sup>41</sup> For a mixed sample, this suggests that an optimum  $T_1$  may be difficult to obtain, and it is important to identify parameters that balance the number of scans to obtain good spectral resolution and relaxation delay time (for kinetic

time-point acquisition). Our experiments demonstrate that conversion calculation with 1 s relaxation delay and 4 scans allows for a representative and accurate quantification ( $R^2 = 1.000$ ) of biodiesel and oil mixtures (Supporting Information, Figure S3 and Table S4). Comparing known mixtures of biodiesel and oil also confirms that our equation gives good correlation and accurate quantification ( $R^2 = 1.000$ , slope = 0.991, Supporting Information, Figure S2).

**Kinetic Studies and Catalyst Comparison.** Initially we selected H<sub>2</sub>SO<sub>4</sub> (0.6 M) as a catalyst to demonstrate the direct real-time monitoring of the transesterification process using NMR spectroscopy. This experiment demonstrated that the time-arrayed NMR method has the ability to monitor the consumption of starting material (TAG) and formation of product (FAMEs) while also indicating the presence of intermediates (e.g., DAGs) (Figures 3 and 4, and Supporting Information, Figure S4). The methine signal from each acylglycerol species is distinctive in the NMR spectra and were integrated for quantification. The presence of an intermediate MAG was unable to be detected. The prevalence of 1,3-DAG over 1,2-DAG seen in the time-array acquisition for transesterification with H<sub>2</sub>SO<sub>4</sub> suggests that either the transesterification is regioselective for the sn-2 position of the TAG, or acyl migration rapidly occurs from the 1,2-DAG to 1,3-DAG, which has been shown with KOH by Jin et al.<sup>42</sup> Previous studies have demonstrated that the methyl ester has a faster rate of formation than acylglycerol depletion.<sup>16</sup> The presence of MAG and the glycerol byproduct were not detected by <sup>1</sup>H NMR spectroscopy in this experiment, either due to low concentration or low solubility in the organic solvent. Typically, transesterification with H<sub>2</sub>SO<sub>4</sub> requires high temperature (100 °C, 3 h); however, for the development of NMR monitoring

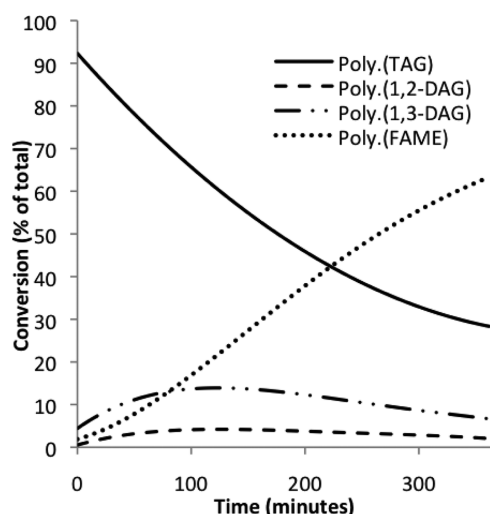


**Figure 3.** Reaction profile analysis of main components present during transesterification with 0.6 M  $\text{H}_2\text{SO}_4$  in fresh reagent-grade methanol (30:1 methanol/oil ratio), performed at 60 °C in  $\text{CDCl}_3$  for 6 h. Data were acquired on a 600 MHz instrument with acquisitions taken every 5 min (8 scans, 45°, 1 s relaxation delay). The integrated glycerol methine represents the conversion of acylglycerols (TAG = 5.27 ppm, 1,3-DAG = 4.09 ppm, 1,2-DAG = 5.08 ppm) and the integrated methyl ester represents the FAME (3.67 ppm). Polynomial line fitting applied to raw data (Supporting Information, Figure S4).

conditions, the reaction was performed at 60 °C to prevent solvent evaporation. Under these reaction conditions, the reaction reaches ~60% completion after 6 h. The water content of the alcohol used for transesterification will also affect the rate of the reaction and the formation of intermediates. Using reagent-grade methanol (previously opened and containing undetermined amounts of water) led to an expected decrease in reaction rate but also an increase in the level of DAG

intermediates observed in the time-array NMR reaction monitoring. We propose that the presence of water facilitates DAG formation and stabilizes the DAG intermediates, which increases the level of intermediates detected during the experiment (Supporting Information, Figure S5).

We have compared reaction monitoring in an NMR tube with aliquots taken from two benchtop reactions (500 mg oil in vials, with and without chloroform solvent) to verify the utility of this method to represent a larger reaction (Supporting Information, Figure S6). The NMR tube reaction was observed to proceed with a faster rate of FAME production and TAG depletion compared to the bench-scale reactions with or without chloroform (i.e., 90% vs 50% conversion in 400 min). Notably, the use of chloroform does not inhibit the reaction and may actually increase the rate of the reaction in both the vial and the NMR tube. The enhanced rate observed for the NMR tube reaction suggests that there is an additional effect from the NMR conditions, such as the narrow shape of the NMR tube, which may facilitate phase separation as the reaction proceeds. This comparison also accentuates the convenience of real-time monitoring using time-array acquisition when compared to manually removing aliquots (followed by washing) throughout the reaction progression.

Transesterification with 1,5,7-triazabicyclo[4.4.0]dec-5-ene (TBD) (Figure 5) was monitored to demonstrate that real-

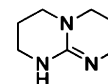


**Figure 5.** 1,5,7-triazabicyclo[4.4.0]dec-5-ene (TBD).

time monitoring with time-array acquisition can be used to compare different catalyst systems. TBD is a bicyclic guanidine base that serves as a bifunctional nucleophilic catalyst for the transesterification of vegetable oil.<sup>43,44</sup>

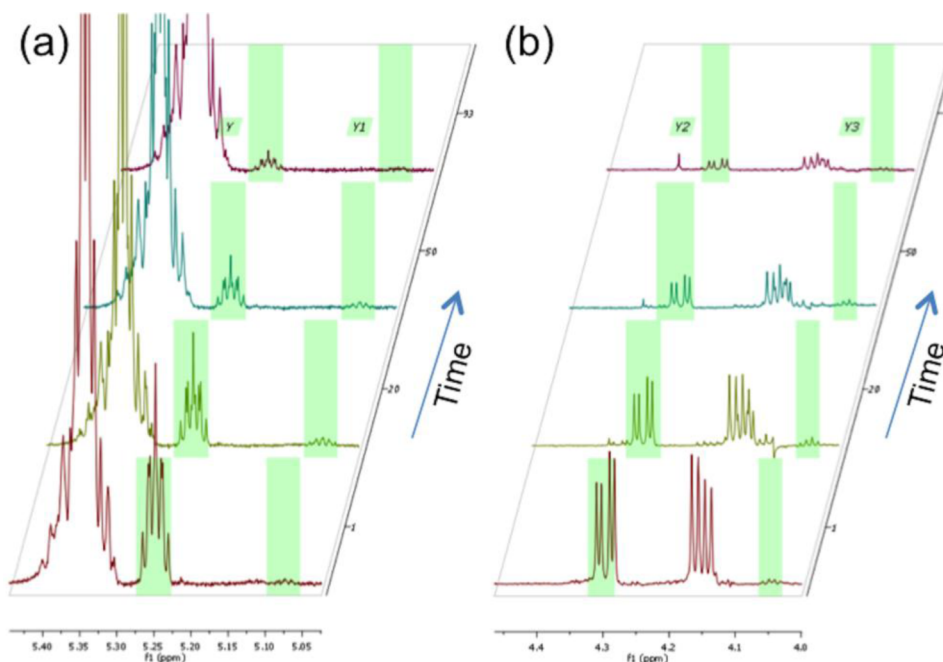


**Figure 4.**  $^1\text{H}$  NMR stacked spectra over time of transesterification with  $\text{H}_2\text{SO}_4$ . (a) Expansion of 5.05–5.45 ppm region. Light green shading signifies area of integration. Y indicates the TAG glycerol methine at 5.27 ppm and Y1 indicates 1,2-DAG glycerol methine at 5.08 ppm. (b) Expansion of 4.00–4.45 ppm. Y2 indicates TAG  $\text{H}_\alpha$  glycerol methylene at 4.29 ppm and Y3 indicates 1,3-DAG glycerol methine at 4.09 ppm.

Catalyst loadings compared for transesterification with TBD include 25, 50, and 100 mol %. Maximum conversion was reached for each catalyst loading within 15 min ranging from 33 to 99% (Figure 6 and Supporting Information, Figure S7).

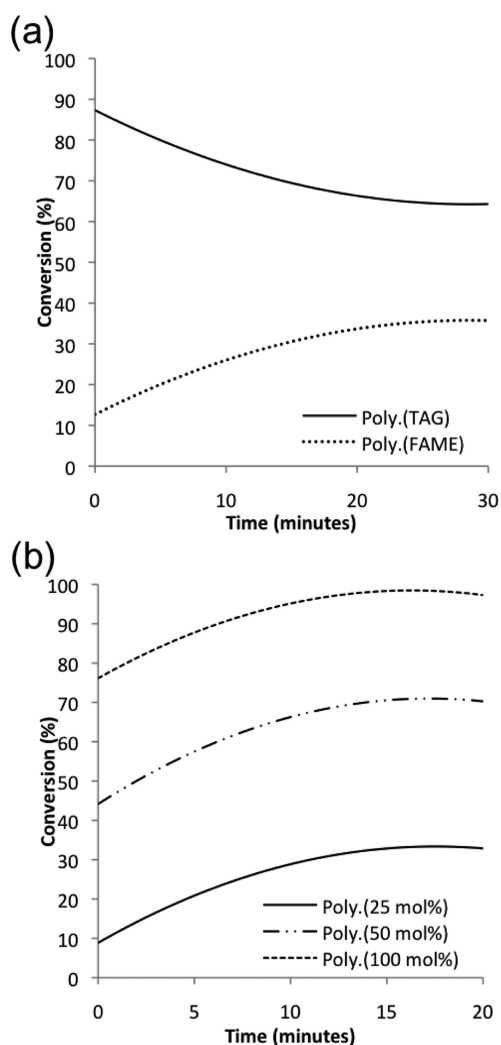


**Figure 6.** (a) Reaction profile of transesterification with 25 mol % of 1,5,7-triazabicyclo[4.4.0]dec-5-ene (TBD) in reagent-grade methanol (30:1 methanol/oil ratio), and (b) kinetic comparison of mol % TBD on FAME conversion. Reaction conditions: olive oil (20 mg) with TBD in reagent-grade methanol, performed at 60 °C in  $\text{CDCl}_3$ . Data were acquired on a Varian 600 MHz spectrometer with acquisitions taken every 2 min (4 scans, 45°, 1 s relaxation delay). The integrated glyceryl methine represents the conversion of acylglycerols (TAG = 5.27 ppm) and the integrated methyl ester represents the FAME (3.67 ppm product). Polynomial line fitting applied (Supporting Information, Figure S8).

DAG and MAG intermediates were not detected in reactions with the TBD catalysis due to very low concentration, which is attributed to a higher reaction rate and alternate mechanism compared to  $\text{H}_2\text{SO}_4$ . Although the literature reports 90% conversion within 1 h at 70 °C with 1 mol % of TBD,<sup>43</sup> using NMR spectroscopic monitoring with TBD required 100 mol % of TBD due to the need for a deuterated solvent for locking the NMR magnetic field, which in turn dilutes substrate interactions. A ratio of 9:1  $\text{CDCl}_3/\text{MeOH}$  gave the best conditions for catalyst solubility and spectral baseline

resolution; however, the increase in methanol required may potentially interfere with the observation of DAG signals.

The real-time monitoring of biodiesel production was also compared with NaOH, a common homogeneous Brønsted base catalyst used for transesterification. TAG disappearance and FAME formation was rapidly observed with maximum conversion after 10 min using 1% (w/w) NaOH at room temperature (Supporting Information, Figure S9).<sup>5</sup> No DAG intermediates were observed in this base-catalyzed reaction, which confirms that the observation of intermediates is dependent on reaction rate and reaction conditions. Initially, higher reaction temperatures were investigated, but the reaction proceeded too quickly to obtain time-array data (>80% and completion with 1% NaOH at 60 °C at first acquisition).

During these NMR experiments, there is also the advantage that the real-time monitoring can provide the opportunity to monitor any changes of the catalyst. For example, real-time monitoring of the TBD-catalyzed transesterification reactions demonstrated a change in the  $^1\text{H}$  NMR signals of the TBD catalyst during the reaction. The observation of such changes in the catalyst signals may provide information about degradation of the catalyst, or may provide mechanistic data. For example, in the case of TBD, the chemical shifts suggest an effect from self-association through hydrogen bonding due to increased temperature when compared in  $\text{CDCl}_3$  and MeOH alone (Supporting Information, Figure S7).

Other advantages of monitoring the transesterification reaction using time-array  $^1\text{H}$  NMR spectroscopy include convenience and efficiency of reaction monitoring in real-time with minimal sampling requirements, real-time analysis of entire reaction mixture with an emphasis on intermediate detection, ability to detect intermediates and prevent incorrect signal integration, and potential to extract kinetic information. The method described here is performed in a standard NMR tube, but it can also be extended for monitoring biodiesel production by flow cell NMR spectroscopy.<sup>45</sup> Potential drawbacks of this method include the use of larger, higher field instruments, which have increased space requirements and costs, and the use of deuterated NMR solvent, albeit in small quantities, which may alter reaction kinetics and composition from solvent interactions and dilution of reaction. While this method allows for direct real-time monitoring on small scale, the method is better considered as a model system because reactions in NMR tubes may proceed with either faster or slower rates, and the use of solvent can dilute substrate interactions relative to the optimized catalyst system used for industrial conditions. Deuterated chloroform was utilized as the NMR solvent for this study because of common availability and solubility of desirable reaction components; however, other deuterated solvents (e.g., acetone, acetonitrile, or THF) may also be have applications for real-time NMR monitoring of acylglycerol transesterification.

## CONCLUSION

Recognizing all of the components present during transesterification is critical when analyzing biodiesel conversion in order to control and quantify purity and prevent errors in calculating conversion. Low magnetic field strengths should be used with caution, as minor components are more difficult to detect due to poor resolution and overlapping peaks can lead to errors in integration assignment. A new equation (eq 3), based on the resolution provided by high magnetic field strength (e.g., 600 MHz), can calculate transesterification conversion with

improved accuracy. The use of NMR spectroscopy in conjunction with time-array acquisition allows for the real-time monitoring of reaction components and can also be extended to investigate solvent effects, additives, and cocatalysts to optimize transesterification conditions.<sup>45</sup> Catalyst activity and reaction optimization may be monitored with greater clarity due to the ability to monitor and detect intermediates, which are often not quantitatively evaluated when aliquots are monitored. These results indicate that time-array <sup>1</sup>H NMR spectroscopy will be valuable for monitoring transesterification catalyst systems for biodiesel production as well as related reactions of acylglycerols with applications in food and pharmaceutical industries.<sup>46</sup>

## ■ ASSOCIATED CONTENT

### Supporting Information

Additional spectra, comparison of biodiesel conversion, relaxation delay comparison, and other data. This material is available free of charge via the Internet at <http://pubs.acs.org>.

## ■ AUTHOR INFORMATION

### Corresponding Author

\*Phone: 530-752-9820. E-mail: [akfranz@ucdavis.edu](mailto:akfranz@ucdavis.edu).

### Notes

The authors declare no competing financial interest.

## ■ ACKNOWLEDGMENTS

This work is supported by Chevron Technology Ventures and the University of California, Davis. A.K.F. acknowledges the 3M Corporation for a Nontenured Faculty award. L.A.A. acknowledges support from the National Science Foundation in the form of a Graduate Research Fellowship and a Bradford Borge Fellowship from UC Davis. We thank Jerry Dallas (UC Davis, NMR Facility) for helpful discussions and advice.

## ■ REFERENCES

- (1) Yusuf, N. N. A. N.; Kamarudin, S. K.; Yaakub, Z. *Energy Convers. Manage.* **2011**, *52*, 2741–2751.
- (2) *International Energy Outlook 2011*, DOE/EIA-0484(2011); U.S. Energy Information Administration: Washington, DC, Sept. 19, 2011.
- (3) Lotero, E.; Liu, Y.; Lopez, D. E.; Suwannakarn, K.; Bruce, D. A.; Goodwin, J. G. *Ind. Eng. Chem. Res.* **2005**, *44*, 5353–5363.
- (4) Jothiramlalingam, R.; Wang, M. K. *Ind. Eng. Chem. Res.* **2009**, *48*, 6162–6172.
- (5) Freedman, B.; Butterfield, R.; Pryde, E. *J. Am. Oil Chem. Soc.* **1986**, *63*, 1375–1380.
- (6) Machado Correa, S.; Arbilla, G. *Atmos. Environ.* **2008**, *42*, 769–775.
- (7) ASTM Standard D6751. *Standard specification for biodiesel fuel blend stock (B100) for middle distillate fuels*; ASTM International: West Conshohocken, PA, 2010.
- (8) Dunn, R. O. *J. Am. Oil Chem. Soc.* **2012**, *89*, 1509–1520.
- (9) Gelbard, G.; Brès, O.; Vargas, R.; Vielfaure, F.; Schuchardt, U. *J. Am. Oil Chem. Soc.* **1995**, *72*, 1239–1241.
- (10) Knothe, G. *J. Am. Oil Chem. Soc.* **2000**, *77*, 489–493.
- (11) Morgenstern, M.; Cline, J.; Meyer, S.; Cataldo, S. *Energy Fuels* **2006**, *20*, 1350–1353.
- (12) Cabeça, L. F.; Marconcini, L. i. V.; Mambrini, G. P.; Azeredo, R. B. V.; Colnago, L. A. *Energy Fuels* **2011**, *25*, 2696–2701.
- (13) Costa Neto, P.; Balparda Caro, M.; Mazzuco, L.; Nascimento, M. J. *Am. Oil Chem. Soc.* **2004**, *81*, 1111–1114.
- (14) Rosset, I. G.; Tavares, M. C. H.; Assaf, E. M.; Porto, A. L. M. *Appl. Catal., A* **2011**, *392*, 136–142.
- (15) Kouame, S.-D. B.; Perez, J.; Eser, S.; Benesi, A. *Fuel Process. Technol.* **2012**, *97*, 60–64.
- (16) Dimmig, T.; Radig, W.; Knoll, C.; Dittmar, T. *Chem. Tech. (Leipzig)* **1999**, *51*, 326–328.
- (17) Casas, A.; Ramos, M. J.; Perez, A.; Simon, A.; Lucas-Torres, C.; Moreno, A. *Fuel* **2012**, *92*, 180–186.
- (18) Fernandes, J. L. N.; de Souza, R. O. M. A.; de Vasconcellos Azeredo, R. B. *Magn. Reson. Chem.* **2012**, *50*, 424–428.
- (19) Ng, S. J. *Am. Oil Chem. Soc.* **2000**, *77*, 749–755.
- (20) Tariq, M.; Ali, S.; Ahmad, F.; Ahmad, M.; Zafar, M.; Khalid, N.; Khan, M. A. *Fuel Process. Technol.* **2011**, *92*, 336–341.
- (21) Ghesti, G. F.; de Macedo, J. L.; Resck, I. S. S.; Dias, J. A.; Dias, S. L. C. U. L. *Energy Fuels* **2007**, *21*, 2475–2480.
- (22) Hincapié, G.; Mondragón, F.; López, D. *Fuel* **2011**, *90*, 1618–1623.
- (23) Freedman, B.; Kwolek, W.; Pryde, E. *J. Am. Oil Chem. Soc.* **1986**, *63*, 1370–1375.
- (24) Plank, C.; Lorbeer, E. *J. Chromatogr. A* **1995**, *697*, 461–468.
- (25) Reddy, S.; Titu, D.; Chadha, A. *J. Am. Oil Chem. Soc.* **2010**, *87*, 747–754.
- (26) Andrade, D. F.; Mazzei, J. L.; d'Avila, L. A. *Rev. Virtual Quim.* **2011**, *3*, 452–466.
- (27) Mueller, J. J.; Baum, S.; Hilterhaus, L.; Eckstein, M.; Thum, O.; Liese, A. *Anal. Chem.* **2011**, *83*, 9321–9327.
- (28) Chuck, C. J.; Bannister, C. D.; Gary Hawley, J.; Davidson, M. G. *Fuel* **2010**, *89*, 457–461.
- (29) Richard, R.; Li, Y.; Dubreuil, B.; Thiebaud-Roux, S.; Prat, L. *Bioresour. Technol.* **2011**, *102*, 6702–6709.
- (30) Knothe, G. *J. Am. Oil Chem. Soc.* **2006**, *83*, 823–833.
- (31) He, B. B.; Van Gerpen, J. H. *Biofuels* **2012**, *3*, 351–360.
- (32) Andrade, D.; Mazzei, J.; Kaiser, C.; d'Avila, L. J. *Am. Oil Chem. Soc.* **2012**, *89*, 619–630.
- (33) Satyarthi, J. K.; Srinivas, D.; Ratnasamy, P. *Energy Fuels* **2009**, *23*, 2273–2277.
- (34) Bernstein, M. A.; Štefinović, M.; Sleight, C. J. *Magn. Reson. Chem.* **2007**, *45*, 564–571.
- (35) Clegg, I. M.; Gordon, C. M.; Smith, D. S.; Alzaga, R.; Codina, A. *Anal. Methods* **2012**, *4*, 1498–1506.
- (36) Nilsson, M.; Khajeh, M.; Botana, A.; Bernstein, M. A.; Morris, G. A. *Chem. Commun.* **2009**, 1252–1254.
- (37) <http://mestrelab.com/software/mnova-nmr/> (Accessed date, August 12, 2012).
- (38) Gao, C.; Xiong, W.; Zhang, Y.; Yuan, W.; Wu, Q. *J. Microbiol. Methods* **2008**, *75*, 437–440.
- (39) Gunstone, F. D.; Harwood, J. L.; Padley, F. B. *The Lipid Handbook*, 2nd ed.; Chapman and Hall: London, 1994.
- (40) Mambrini, G. P.; Ribeiro, C.; Colnago, L. A. *Magn. Reson. Chem.* **2012**, *50*, 1–4.
- (41) Socha, A. M.; Kagan, G.; Li, W.; Hopson, R.; Sello, J. K.; Williard, P. G. *Energy Fuels* **2010**, *24*, 4518–4521.
- (42) Jin, F.; Kawasaki, K.; Kishida, H.; Tohji, K.; Moriya, T.; Enomoto, H. *Fuel* **2007**, *86*, 1201–1207.
- (43) Schuchardt, U.; Vargas, R. R. M.; Gelbard, G. *J. Mol. Catal. A: Chem.* **1995**, *99*, 65–70.
- (44) For mechanistic details, see (a) Pratt, R. C.; Lohmeijer, B. G. G.; Long, D. A.; Waymouth, R. M.; Hedrick, J. L. *J. Am. Chem. Soc.* **2006**, *128*, 4556–4557. (b) Kiesewetter, M. K.; Scholten, M. D.; Kirn, N.; Weber, R. L.; Hedrick, J. L.; Waymouth, R. M. *J. Org. Chem.* **2009**, *74*, 9490–9496. (c) Simon, L.; Goodman, J. M. *J. Org. Chem.* **2007**, *72*, 9656–9662.
- (45) Khajeh, M.; Bernstein, M. A.; Morris, G. A. *Magn. Reson. Chem.* **2010**, *48*, 516–522.
- (46) Feltes, M.; de Oliveira, D.; Block, J.; Ninow, J. *Food Bioprocess Technol.* **2012**, DOI: 10.1007/s11947-012-0836-3.